WEAK DOUBLE LAYERS IN THE AURORAL IONOSPHERE

M. K. Hudson, T. L. Crystal, and W. Lotko
Physics and Astronomy Department
Dartmouth College
Hanover, New Hampshire 03755, U.S.A.

and

C. Barnes
Los Alamos National Laboratory
Los Alamos, New Mexico 87545, U.S.A.

ABSTRACT

Previous work on the evolution of weak double layers in a hydrogen plasma has been extended to include H^+ and O^+ with relative drift. It has been shown (Bergmann and Lotko, 1986) that the relative drift between hydrogen and oxygen ions due to a quasi-static parallel electric field gives rise to a strong linear fluid instability which dominates the ion-acoustic mode at the bottom of the auroral acceleration region. This ion-ion instability can modify ion distributions at lower altitudes and the subsequent nonlinear evolution of weak double layers at higher altitudes in the ion-acoustic regime. We have found that ion hole formation can occur for smaller relative electron-ion drifts than seen in previous simulations, due to the hydrogen-oxygen two-stream instability. This results in local modification of the ion distributions in phase space, and a partial filling of the valley between the hydrogen and oxygen peaks, which would be expected at higher altitudes on auroral field lines. It is shown that the observed velocity diffusion does not necessarily preclude ion hole and double layer formation in hydrogen in the ion-acoustic regime. These simulation results are consistent with the experimentally measured persistence of separate hydrogen and oxygen peaks, and the observation of weak double layers above an altitude of 3000 km on auroral field lines.

I. INTRODUCTION

Weak double layers with potential jumps comparable to the electron thermal energy have been observed to form in one-dimensional (Sato and Okuda, 1980) and two-dimensional (Barnes et al., 1985) electrostatic particle simulations; the double layer formation is driven by an electron drift relative to ions which is unstable to the ion-acoustic mode but is less than the electron thermal speed. Such weak double layers have been observed in space in the auroral particle acceleration region (Temerin et al., 1982), and in laboratory plasmas (Chan et al., 1984; Sekar and Saxena, 1985; Chan, 1986). Thus far, theoretical efforts at understanding weak double layer formation have focussed on a single ion species, while it is known from space observations that weak double layers occur in regions of upward flowing hydrogen and oxygen of ionospheric origin. A quasi-static parallel electric field has been postulated to explain the observed particle distributions (Chiu and Schulz, 1978; Lyons, 1980). While the existence of such a field will remain a zeroeth order assumption in the present paper, we will also examine non-adiabatic modifications of the particle distributions at the bottom of the acceleration region which may affect weak double layer evolution further up the field line, and the stability of the assumed quasi-static field.

We will first briefly review previous work on weak double layer evolution in a hydrogen plasma, and then extend our simulations to include a relative drift between hydrogen, oxygen, and electrons which occurs, for example, in a mirror-supported parallel electric field. Our purpose is to examine the nonlinear effects of the resulting hydrogen-oxygen two-stream instability (Bergmann and Lotko, 1986) on the particle distributions, and consequences for double layer formation further up the field line.

III. WEAK DOUBLE LAYER FORMATION IN A HYDROGEN PLASMA

Barnes et al. (1985) showed in a series of one- and two-dimensional, bounded and periodic particle simulations that weak double layers with potential jumps comparable to the electron thermal energy form when the system is driven by an electron drift relative to ions which is less than the electron thermal speed, e.g., $V_d = 0.5 - 0.7\ a_e$, and an electron to ion temperature ratio $T_e/T_i >> 1$. The electron drift was maintained by injection of electrons from the boundaries at a continuous rate in bounded runs, and by applying a weak electric field uniformly across the system in periodic runs.

Sato and Okuda (1980) first studied the occurrence of weak double layers in a one-dimensional periodic system in which electrons are given an initial drift that subsequently decays. They found that it was necessary to use a long system, $L > 256\ \lambda_D$ (Debye lengths), in order for weak double layers to form in periodic runs. Our subsequent interpretation (Barnes et al., 1985) is that long periodic systems are required to prevent electron recycling from the low to high potential side, which neutralizes the double layer. Electron injection boundary conditions eliminate this problem in bounded simulation runs, and a weak applied electric field acts to impede electron recycling in periodic runs; both of these simulation techniques allow shorter system lengths.

Figure 1 from Barnes et al. (1985) shows the temporal evolution and recurrence of weak double layers in a one-dimensional system with electron injection boundaries. Ion-acoustic turbulence evolves, for $V_H = 0.5\ a_e$ and $T_e/T_i = 50$, into a discrete localized pulse which propagates into the system initially at the sound speed. The pulse is characterized by a negative potential dip which amplifies by momentum exchange with reflected electrons (Lotko, 1983; Chanteur et al., 1983); the asymmetic reflection of electrons results in a potential jump downstream. As the negative potential dip grows, it traps ions, slowing down the pulse via mass loading until an effective Bohm criterion for existence of the double layer potential jump is no longer met. The latter requires that ions flow into the high potential side at or near the sound speed (Chen, 1974), achieved here by motion of the pulse in the ion frame. The potential jump then decays and ion holes (Chan, 1986) or ion-acoustic solitons (Sato and Okuda, 1981) propagate away from the high potential side to seed new double layer formation. The decaying ion hole, still apparent in phase space, recoils backward as it moves downward through the ion distribution.

Barnes et al. (1985) examined the persistence of weak double layers in two-dimensional magnetized simulations. Electron injection boundary conditions produce one-dimensional double layers which are roughly uniform across the system in the direction perpendicular to **B**. To examine the transverse scale, a doubly periodic system with a weak electric field imposed uniformly along **B** was employed. The magnitude of the electric field was such that the corresponding potential drop across the system was less than the electron thermal energy, or $eE_o/T_e = 0.6/160\ \lambda_D$. Figure 2 shows transverse localization of weak double layers for strongly magnetized electrons ($\omega_{ce}/\omega_{pe} = 3$ is the ratio of electron gyro to plasma frequency). The transverse dimension appears to decrease with increasing magnetic field strength, scaling with $\sqrt{\lambda_D^2 + \rho_s^2}$, where λ_D is the Debye length and ρ_s is the ion gyroradius at the electron temperature. The parallel scale length remains the order of tens of Debye lengths, as in one-dimensionality. Ion-acoustic turbulence becomes homogeneous and does not evolve into localized weak double layers in weakly magnetized ($\omega_{ce}/\omega_{pe} < 1$) periodic systems. One therefore might expect to see such structures in the auroral acceleration region, but not, for example, in the solar wind.

IV. ION HOLES IN MULTIPLE ION SPECIES PLASMAS

To the double layer evolution problem we would now like to add the effects of multiple ion species, H^+ and O^+, with relative drift. This introduces an important complication noted by Bergmann and Lotko (1986). A quasi-static parallel electric field produces a relative drift between ionospheric hydrogen and oxygen ions which have been accelerated through the same potential drop, such that $V_H/V_O = \sqrt{M_O/M_H} = 4$. This situation is fluid unstable for parallel propagating modes when the relative H^+-O^+ drift exceeds a minimum, determined primarily by ion Landau damping, up to a maximum value that is less than about twice the hydrogen sound speed $C_s = \sqrt{T_e/M_H}$. This indicates that the ion two-stream instability (for parallel propagating waves) will be confined to the bottom of the acceleration region, since at higher altitudes the relative drift will exceed the upper bound for instability. It is likely, although it has not yet been demonstrated, that obliquely propagating modes may still be unstable for drifts exceeding this upper bound. The growth rate for the ion two-stream instability is larger than that for typical (electron-ion) current-driven instabilities, and one might expect significant modifications of the hydrogen and oxygen distributions to occur. In particular, the unstable ion two-stream waves have phase velocities lying between the hydrogen and oxygen distributions, and one might expect some quasi-linear filling, that is to say, formation of tails on the high and low velocity sides of oxygen and hydrogen, respectively. This quasi-linear filling could, in turn, affect the ion-acoustic instability and double layer evolution at higher altitudes, when ion drifts relative to electrons become a significant fraction of the electron thermal speed, as required for double layer formation in hydrogen plasma simulations. The instability analysis and simulations require knowledge or assumptions about the electron distribution in the region of interest. Bergmann and Lotko (1986) have integrated the electron distribution functions, $F(v_\parallel, v_\perp)$, in the Chiu-Schulz (1978) equilibrium model of a mirror-supported electric field to obtain an effective one-dimensional distribution, $f(v_\parallel)$. These electron populations include precipitating magnetospheric electrons, primary and secondary backscattered electrons, and those electrons which are trapped between the magnetic mirror below and retarding electrostatic potential above. At an altitude relevant to the ion two-stream instability, the bulk of ionospheric electrons has been retarded at lower altitudes by the potential drop which produces the relative ion drifts. The sum of the remaining electron populations, shown in Figure 3, is essentially a stationary Maxwellian with a precipitating electron tail. Also shown in the figure is a Maxwellian fit for the first three moments as described by Bergmann and Lotko.

We would like to examine the spatial evolution of the ion distribution functions along the geomagnetic field line at various distances above the bottom of the acceleration region (nominally at an altitude of 2000 km in Chiu and Schulz, 1978), including the ion two-stream unstable regime near the bottom on up to altitudes where the ion drifts become comparable to the electron thermal speed, and where double layers have been observed (>3000 km altitude). Since our computer resources limit the simulation system to lengths less than or the order of 1000 Debye lengths, we examine instead a temporal evolution problem which differs from the spatial evolution problem in at least one respect. In the spatial evolution case, the ratio of the H^+/O^+ bulk drift velocity is $\sqrt{M_O/M_H}$, as oxygen and hydrogen are accelerated to the same energy as a function of potential at a given altitude. In steady state at a fixed altitude there will be a continuous flow of oxygen and hydrogen whose drifts differ by a factor of 1 to 4, respectively, but the hydrogen and oxygen ions passing that altitude at a fixed time will not leave the bottom of the acceleration region simultaneously, since hydrogen flows up the field line faster. This follows from the relation

$$e\phi = 1/2\, M_H V_H^2 = 1/2\, M_O V_O^2 \quad , \tag{1}$$

which holds at any given altitude where the potential is $e\phi$. Alternatively, in a simulation system evolving in time with a uniformly applied E_o, the ion velocity varies as

$$V_i = \frac{eE_o t}{M_i}$$

which results in an H^+–O^+ velocity of M_O/M_H, rather than $(M_O/M_H)^{1/2}$. Furthermore, depending on the strength of the applied electric field E_o, the ions may accelerate so rapidly that the upper limit on the relative drift for the ion two-stream instability may be exceeded before nonlinear saturation can occur. In such a case, we would not see the full effects of wave-particle interactions on the ion distributions.

With these caveats in mind, we performed a series of one-dimensional electrostatic simulations using the particle code ES1 (Birdsall and Langdon, 1984), in a periodic system of length 240 λ_D, using 16,000 hydrogen and 16,000 oxygen ions and 32,000 electrons. We varied the uniform applied electric field from $eE_o/T_e = 0$, 1.2/240 λ_D to 2.4/240 λ_D and applied it only to the ions in order to simulate the approximately stationary electron Maxwellian (Fig. 3) through which the outflowing ions accelerate. We did initial value runs with $V_H = V_O = O$ at t = O and runs which were initiated with V_H and V_O in the range where the ion two-stream growth rate peaks.

Figure 4 shows the nonlinear evolution of the ion two-stream instability for initial drifts $V_H = 1.2\,C_s$ and $V_O = 0.3\,C_s$ and a uniform applied electric field $eE_o/T_e = 2.4/240\,\lambda_D$. The electron-to-ion temperature ratio is $T_e/T_i = 20$ and the mass ratios are $M_H/M_e = 50$ and $M_O/M_H = 8$. The choice of drifts $V_H/V_O = 4$ is intermediate between the spatial evolution case where $V_H/V_O = \sqrt{M_O/M_H} = 2\sqrt{2}$ and the temporal evolution case where $V_H/V_O = M_O/M_H = 8$ for our mass ratio. Variations about this set of parameters are discussed below. One observes the formation of a localized fluctuation in the potential similar to that seen in the previously described (single ion) simulations at a time when the hydrogen drift relative to electrons is $V_H = 0.2$-$0.3\,a_e$. This drift is smaller by a factor of 2 than in the single ion runs previously shown. The localized wave is a result of the nonlinear evolution of the ion two-stream instability which occurs at lower relative drifts (V_H-V_O) than the current-driven, ion-acoustic instability. The potential pulse is subsonic in the ion frame, and appears to propagate with the ions out the right-hand boundary and re-enter on the left. Periodicity of the system allows one to see that the pulse is continuous from the right through the left boundary of an adjacent frame, since the pulse has not moved much from frame to frame. (The frames are separated in time by 60 ω_{pe}^{-1}.) A significant localized potential jump $e\phi/T_e \gtrsim 1$ develops, but does not persist as far downstream as in cases where the relative electron-ion drift is larger (Fig. 11). We therefore hesitate to call this structure a double layer when the system is in the ion two-stream unstable regime, although its features are very similar to those shown in Figure 1, when translated to a frame in which electrons are stationary and ions drift. One sees trapping of hydrogen and oxygen on the sides of the distribution functions corresponding to the phase velocities of the (ion two-stream) unstable waves, namely the low velocity side of hydrogen and the high velocity side of oxygen. It seems appropriate to call this structure an ion hole.

We observed ion hole formation in the ion two-stream unstable regime for a range of parameters summarized in Table 1. The ion two-stream instability was observed over a broader range of parameters (Bergmann and Lotko, 1986) than was ion hole formation, which apparently requires large amplitude waves and occurs only for sufficiently rapid linear instability. Recall that the ion two-stream instability is limited in duration as the electric field accelerates ions into and out of the range of linearly unstable drifts. Ion hole formation did not occur in runs 2-4 until the hydrogen bulk was accelerated to 0.2-0.3 a_e. In run 6, with no applied electric field but the same initial drifts as run 3, ion hole formation was not observed. In run 7, also with no electric field, but with initial drifts in the range produced by the electric field in run 3 at the time ion hole formation was observed, an ion hole forms. Sato and Okuda (1980) saw weak double layer formation in a system 256 λ_D long but not in one 128 λ_D long. Our system length of 240 λ_D is marginally long enough to allow a double layer to form in the absence of an applied electric field before periodic electron cycling neutralizes the evolving double layer space charge. We also did a run (8) using a bounded one-dimensional electrostatic code, PDW1 (Lawson, 1984), with constant particle injection maintained by an external circuit and floating potential at both ends of the system, but with parameters otherwise the same as in run 7. Ion hole formation in runs 7 and 8 is comparable, as shown in Figure 5.

In order to address the temporal evolution question, we performed two runs (9 and 10) with two different values of the applied electric field, $eE_o/T_e = 1.2, 2.4/240\ \lambda_D$, no initial ion drifts, and periodic boundary conditions. Ion hole formation was evident but weaker for the larger electric field (run 9) than in the initial drift case (e.g., run 3), and absent for the weaker electric field (run 10) when compared at time such that $C_s < V_H\text{-}V_O < 2\ C_s$. Some ion heating occurs in the initial value runs (9 and 10) before the relative drifts are comparable to the initial drift runs, i.e., optimum for ion two-stream instability. In initial value runs the hydrogen and oxygen ion distributions separate more quickly than in the case of spatial evolution, and so spend less time in the range of unstable relative drifts, $V_H - V_O \lesssim 2\ C_s$. The maximum growth rate of the two ion-stream instability is the order of $\gamma/\omega_{pe} \sim 10^{-2}$ (Bergmann and Lotko, 1986, Fig. 3) for the k modes in our simulation system of length 240 λ_D and grid size 0.5 λ_D. Both initial value (run 9) and initial drift (run 3) cases remain in the range of unstable drifts $V_H\text{-}V_O \sim 1.2\text{-}2\ C_s$ a number of e-folding times, but there appears to be some difference between initializing the system in the linearly unstable regime and evolving through it. In the auroral problem, one expects spatial evolution and weaker electric fields, discussed below, to separate the drifts more slowly relative to the linear growth time.

The question arises whether ion heating by the ion two-stream instability, evident in Figure 4, will affect double layer evolution at higher altitudes where the ion drift relative to electrons is larger. Figure 6 shows the initial ion and electron distributions for runs 9 and 10. Figure 7 shows the same distributions for run 9 at the time an ion hole is beginning to form, while Figure 8 shows the same distributions at a later time when the hydrogen drift is becoming significant relative to electrons. Figure 9 shows the particle distributions in the weaker electric field case at a time when the drift is the same as Figure 7. We would conclude from this set of figures tht there is no major modification of the hydrogen and oxygen distributions by the ion two-stream instability, which is present in runs 9 and 10. There is some heating on the low velocity side of hydrogen and the high velocity side of oxygen, as expected, in the range of unstable ion two-stream phase velocities. Figure 10, a similar plot for run 3 which showed ion hole formation at large trapping amplitudes ($e\phi/T_e \sim 1$), indicates more heating between the hydrogen and oxygen distributions. This plot exhibits distribution functions which are spatially averaged across the whole system, and it is the case that the plateau evident in hydrogen (and oxygen) is due primarily to the spatially localized ion hole evident in Figure 3. It is questionable to call this heating versus localized ion trapping since it is not uniform across the system. It therefore seems reasonable to conclude that in our simulation system the hydrogen and oxygen average distributions are not so greatly modified by the ion two-stream instability as to preclude ion-acoustic instability and double layer formation at larger ion drifts relative to electrons.

IV. ION-ACOUSTIC DOUBLE LAYERS IN AN O^+-H^+ PLASMA

As hydrogen and oxygen continue to accelerate up the geomagnetic field line out of the region of ion two-stream instability, hydrogen eventually acquires a drift relative to electrons comparable to the electron thermal speed. If the hydrogen velocity distribution has not been too greatly modified by the ion two-stream instability, as our preceding results indicate, we might expect double layers to evolve from the electron-hydrogen acoustic instability, as described by Barnes et al. (1985), as long as oxygen and hydrogen remain well separted. To test this, we did a series of simulations at large electron drifts (0.7-0.9 a_e) in the oxygen frame with hydrogen drifting at -0.2 C_s. Electron injection boundary conditions were employed as in Barnes et al. (1985), in a system 512 λ_D long, containing 8000 ions of each species and 16,000 electrons. More realistic mass ratios, $M_H/M_e = 1000$ and $M_O/M_H = 10$, were used. Oxygen was kept cold relative to electrons, $T_e/T_O = 100$, and two cases were examined for hydrogen: $T_e/T_H = 20$ corresponding to no significant heating of hydrogen by the ion two-stream instability at lower altitudes, and $T_e/T_H = 2$ where significant heating has occurred. The assumption that electrons are hotter than ions is justified by the altitude where weak double layers have been observed (>3000 km), since the large scale parallel electric field restricts colder electrons to lower altitudes. No electric field was applied in these bounded runs.

Figure 11 shows the hydrogen and oxygen distributions and potential at a time when one and possibly a second double layer are forming with hole(s) evident in hydrogen phase space. Oxygen responds more slowly and appears to play a passive role in the double layer formation, but eventually forms a hole in ion-phase space by the time hydrogen has undergone significant heating and the double layer is disappearing (Fig. 12). In a similar run with $T_e/T_H = 2$, a hole does not appear to form in hydrogen but is evident in oxygen at later times. This result is consistent with Schamel's (1982) criterion that ion holes do not form for $T_e/T_i < 3.5$ (see also Hudson et al., 1983). An oxygen ion hole and weak double layer appear to form when the hydrogen is heated too much to support such a structure. Should the hydrogen be significantly heated and the oxygen remain cool, a hole can still form in oxygen in association with an electron -O^+ drift instability at phase velocities between the electron and O^+ peaks.

V. APPLICATION TO THE AURORAL REGION

A number of caveats are in order before applying the foregoing simulation results to the auroral particle acceleration region. We have examined separately two regimes: (1) where the two ion-stream instability operates at low relative ion drifts ($<2\ C_s$) produced by a quasi-static parallel electric field near the bottom of the acceleration region, and (2) ion-acoustic double layer formation at higher altitudes where relative electron-ion drifts are larger and the ion distributions will have undergone some heating at lower altitudes. We have restricted our analysis to parallel propagating modes and one-dimensional simulations in the present paper. It is likely that oblique modes will affect the ion distributions. Kaufmann et al. (1986) have examined the stability of hydrogen and oxygen beams measured by the S3-3 and DE 1 satellites and concluded that oblique modes are unstable. It may also be the case that the upper limit on relative drift for the ion two-stream instability is relaxed for oblique modes, since $\hat{\mathbf{k}} \cdot (\mathbf{V}_H - \mathbf{V}_O) < 2\ C_s$ for larger relative ion drifts when $\mathbf{k}$ is oblique. The linear instability of oblique modes is under investigation by Bergmann (private communication, 1986). Barnes et al. (1985) showed that ion-acoustic double layers evolve in the presence of oblique (EIC) modes in two-dimensionality with behavior similar to the one-dimensional case. We plan to extend the present multi-ion studies to two-dimensional in the future.

Another qualification to our conclusions is the strength of the electric field used in the initial value simulations. The values of $eE_o/T_e = 1.2\text{-}2.4/240\ \lambda_D$ correspond to 5-10 mV/m for $\lambda_D = 10$ m, $T_e = 10$ eV, and $n_e = 10$ cm^{-3}. These are not large parallel electric fields compared with observations in the acceleration region (Temerin, private communication, 1986), but are larger than the mirror-supported fields calculated by Chiu and Schulz (1978) which maximize at $E_o < 0.5$ mV/m near the bottom of the acceleration region.

It is somewhat difficult to extrapolate from the temporal evolution approach taken in this paper to the spatial evolution of ion distributions along auroral field lines. Nonetheless, with the neglect of oblique modes and use of somewhat large electric fields, and/or initializing the simulations with unstable drifts, and preheated ions in the ion acoustic regime, we find the following:

1. Ion holes form in the ion two-stream unstable regime at relatively low drifts compared with those required to form ion-acoustic double layers. They occur in systems with and without an applied electric field, but over a narrow range of relative hydrogen-oxygen drifts.

2. The ion two-stream instability does not appear to greatly modify the ion distributions, except locally in the presence of a large amplitude ($e\phi/T_e \sim 1$) ion hole.

3. Double layer evolution should proceed at higher altitudes as previously described in the ion-acoustic regime, with holes forming in hydrogen, and oxygen responding passively.

There are two pieces of experimental evidence supporting our conclusion that hydrogen and oxygen distributions are not so greatly modified at lower altitudes by the ion two-stream instability as to preclude double layer formation at higher altitudes.The first is the set of particle measurements from the S3-3 and DE 1 satellites analyzed by Kaufmann et al. (1986) showing well separated H^+ and O^+ peaks, with a slight filling in between the two. The second is the observation of what have been identified as weak double layers by Temerin et al. (1982), also Temerin and Mozer (1986), at altitudes >3000 km in regions of upward ion flows. These observations indicate that the heating of the ion distributions that occurs at lower altitudes is not as great as the relative acceleration, nor enough to make $T_e/T_i \sim 1$, which would preclude ion-acoustic double layer formation.

A number of questions remain to be addressed: Can one design a temporal evolution simulation which better models the spatial evolution problem within the constraints of computer time and memory, e.g., by moving one ion species with an electric field which differs from the other by $\sqrt{M_H/M_O}$ to mimic the spatial case in an initial value problem? What effects do oblique modes and two-dimensionality introduce in the problem? Is it possible to use weaker electric fields and follow the evolution from the ion two-stream through the ion-acoustic double layer regime. These and other questions remain to be addressed in future work on the evolution of weak double layers in the multi-species auroral plasma.

TABLE 1. ION HOLE FORMATION IN THE ION TWO-STREAM UNSTABLE REGIME

Run	$V_O(0)$ (a_e)	$V_H(0)$ (a_e)	V_H-V_O (C_s)	eE_o/T_e	bc	t (ω_{pe}^{-1})	hole
1	0	0.17	1.2	2.4	per	0	no
2	0.035	0.17	0.95	2.4	per	0	yes
3	0.042	0.17	0.91	2.4	per	0	yes
4	0.049	0.17	0.86	2.4	per	0	yes
5	0.06	0.17	0.78	2.4	per	0	no
6	0.042	0.17	0.91	0	per	0	no
7	0.06	0.30	1.7	0	per	0	yes
8	0.06	0.30	1.7	0	bnd	0	yes
9	0	0	0	2.4	per	0	marginal
10	0	0	0	1.2	per	0	no

Note: Units of eE_o/T_e are $(240\ \lambda_D)^{-1}$; bnd and per refer to bounded and periodic boundary conditions (bc).

Acknowledgments. This research was supported by NSF grant ATM-8445010, the University of California IGPP Award No. 100, and the U. S. Department of Energy. T. L. Crystal was also supported by a grant from the Andrew Mellon Foundation.

REFERENCES

Barnes, C., M. K. Hudson, and W. Lotko, *Phys. Fluids, 28,* 1055 (1985).

Bergmann, R. A., and W. Lotko, *J. Geophys. Res.*, in press, 1986.

Birdsall, C. K., and A. B. Langdon, *Plasma Physics via Computer Simulations,* McGraw Hill, New York, 1984.

Chan, C., these proceedings, 1986.

Chan, C., M. H. Cho, N. Hershkowitz,, and T. Intrator, *Phys. Rev. Lett., 52,* 1782 (1984).

Chanteur, G. J., C. Adam, R. Pellat, and A. S. Volokhitin, *Phys. Fluids, 26,* 1584 (1983).

Chen, F. F., *Introduction to Plasma Physics,* Plenum, New York, 1974.

Chiu, Y. T., and M. Schulz, *J. Geophys. Res., 83,* 629 (1978).

Hudson, M. K., W. Lotko, I. Roth, and E. Witt, *J. Geophys. Res., 88,* 916 (1983).

Kaufmann, R. L., G. R. Ludlow, H. L. Collin, W. K. Peterson, and J. L. Burch, *J. Geophys. Res.*, submitted, 1986.

Lawson, W. S., *PDW1 Users Manual,* Memorandum No. UCB/ERL M84/37, University of California, Berkeley, 1984.

Lotko, W., *Phys. Fluids, 26,* 1771 (1983).

Lyons, L. R., *J. Geophys. Res., 85,* 17 (1980).

Sato, T., and H. Okuda, *Phys. Rev. Lett., 44,* 740 (1980).

Sato, T., and H. Okuda, *J. Geophys. Res., 86,* 3357 (1981).

Schamel, H., *Symposium on Plasma Double Layers,* Riso (1982).

Sekar, A. N., and Y. C. Saxena, *Plasma Phys. and Cont. Fusion, 27,* 181 (1985).

Temerin, M., and F. S. Mozer, these proceedings, 1986.

Temerin, M., K. Cerny, W. Lotko, and F. S. Mozer, *Phys. Rev. Lett., 48,* 1175 (1982).

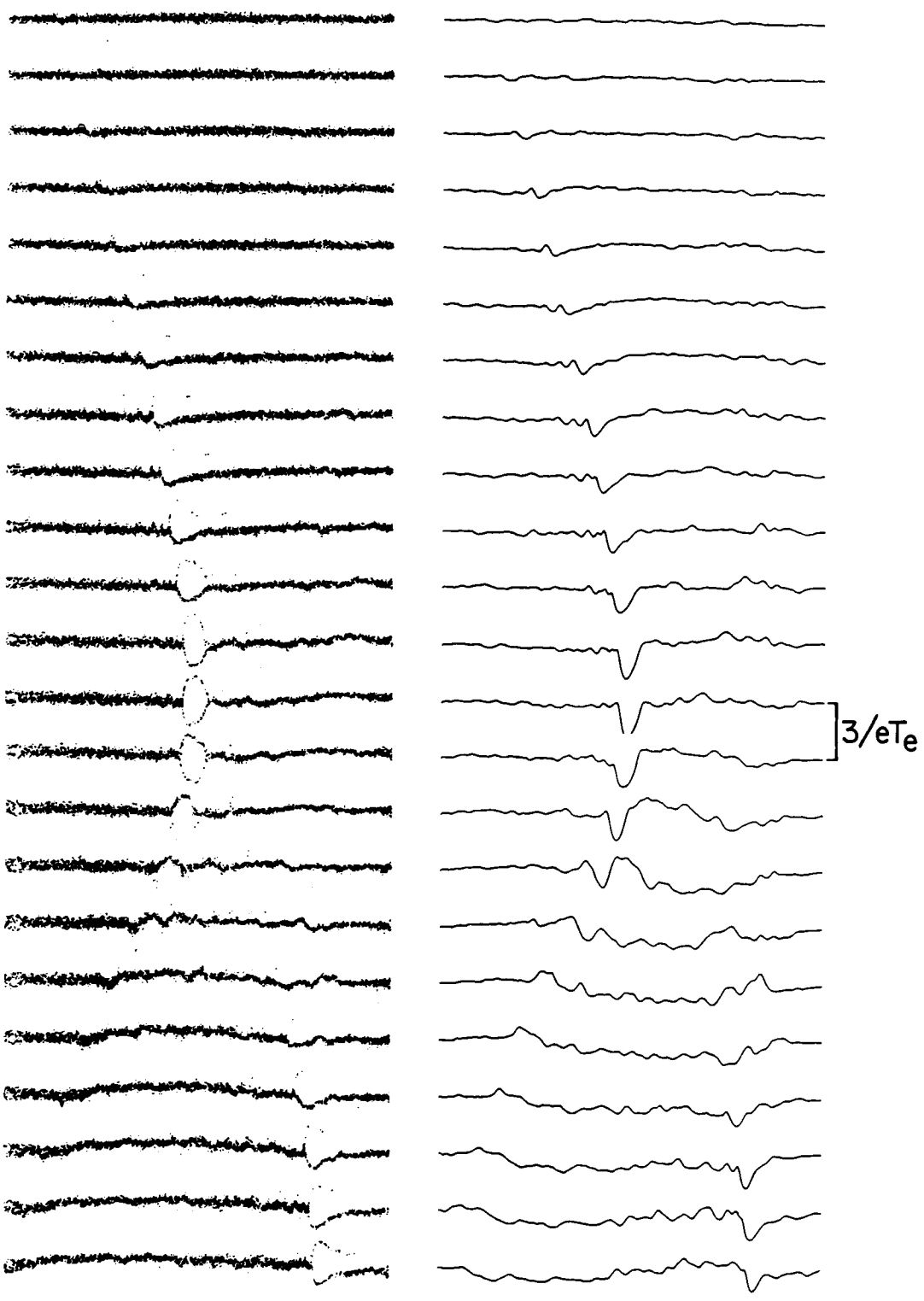

Figure 1. Time series plots of ion-phase space (left) and electrostatic potential (right) for a bounded one-dimensional run with M/m = 2000, T_e/T_i = 50, and V_H = 0.5 a_e. The snapshots are taken at intervals of 360 ω_{pe}^{-1} (8 ω_{pi}^{-1}) beginning at 1080 ω_{pe}^{-1} (24 ω_{pi}^{-1}) (from Barnes et al., 1985).

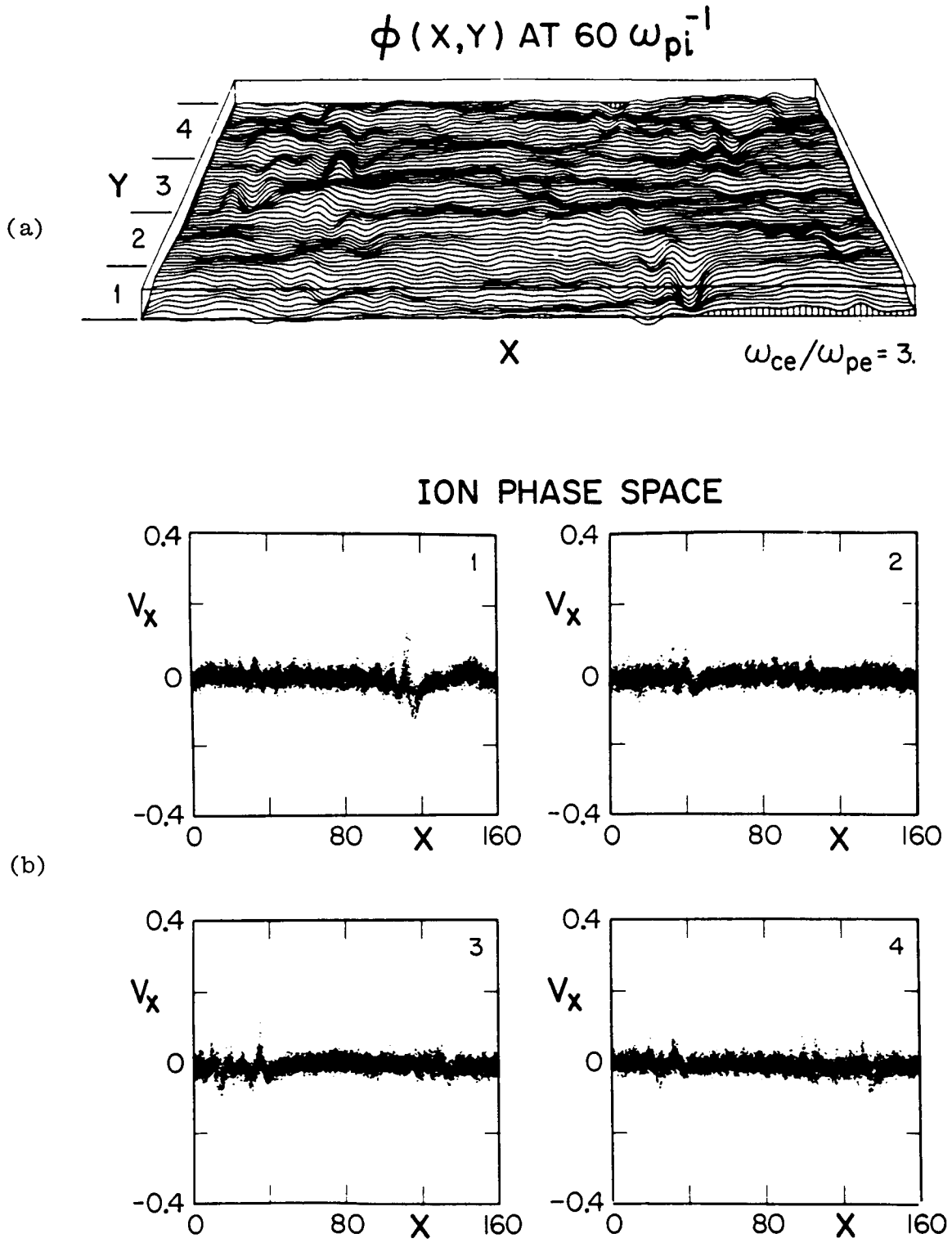

Figure 2. Magnetized doubly periodic system with $\omega_{ce}/\omega_{pe} = 3$ and a weak uniform applied electric field pointing to the left, $eE_o/T_e = 0.6/160\ \lambda_d$. (a) Potential profiles are averaged over 4 ω_{pi}^{-1}; (b) ion-phase space v_x versus x is displayed in each of four bands in y. v_x is in units of a_e. The most prominent double layers are in band 1 at $x \approx 120\ \lambda_D$ and band 3 at $x \approx 40\ \lambda_D$.

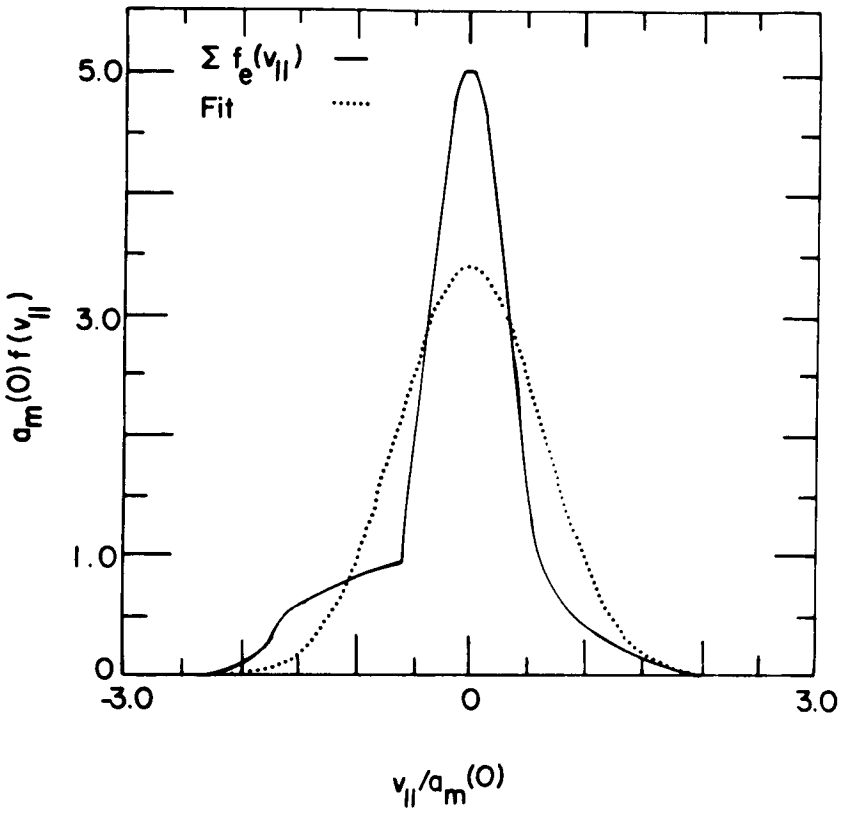

Figure 3. Reduced electron distribution function f(V) for Chiu and Schulz (1978) Model W, at $e\phi/T_c = 110$, where T_c is the cold ionospheric electron temperature. This represents a sum of contributions from magnetospheric, primary and secondary backscattered and trapped electrons, with ionospheric electrons negligible at this value of the mirror potential measured from zero at an altitude of 2000 km (adapted from Bergmann and Lotko, 1986).

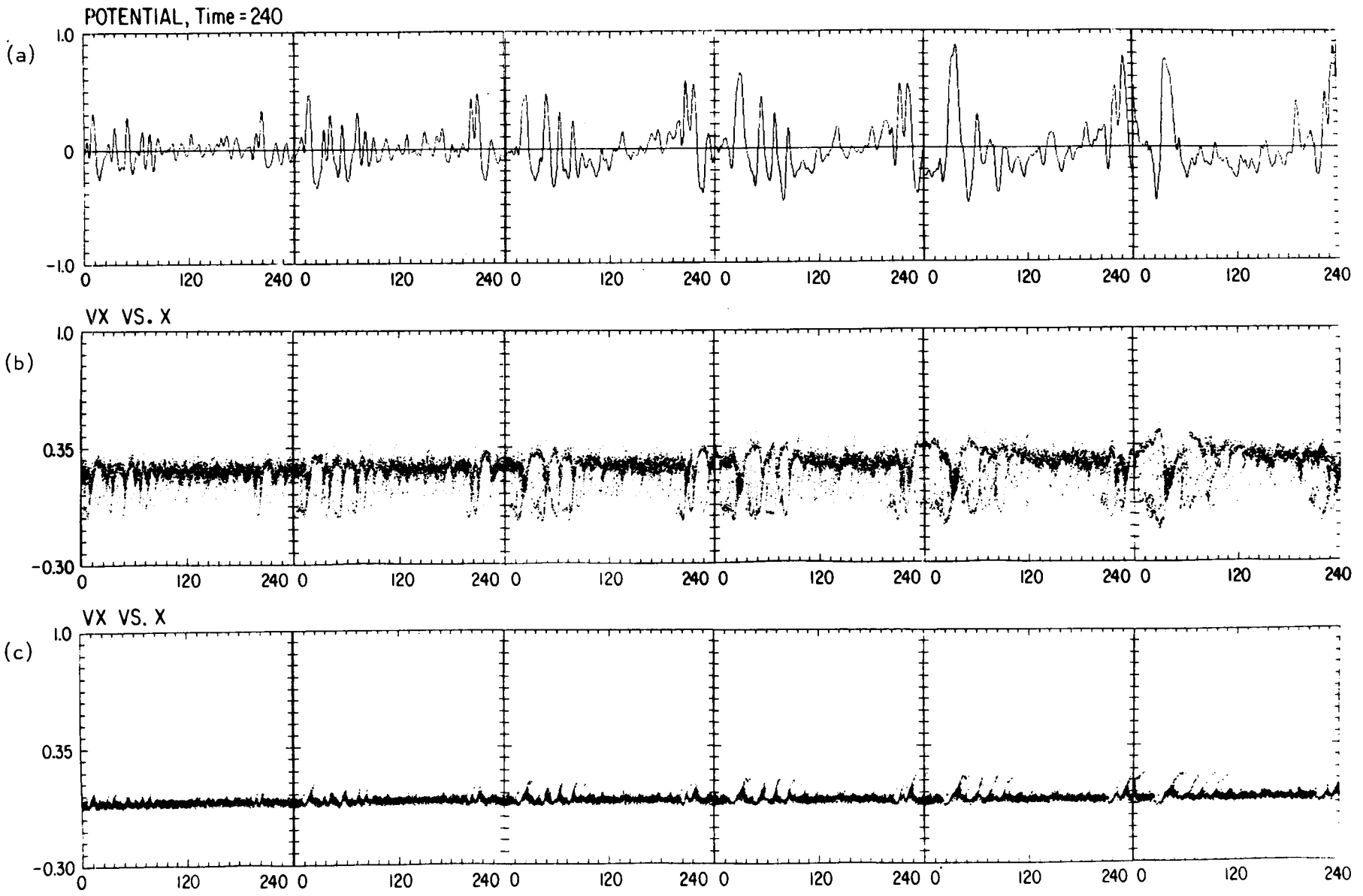

Figure 4. Run 3, Table 1. Time evolution from left to right of (a) the electrostatic potential every 60 ω_{pe}^{-1} averaged over 30 ω_{pe}^{-1} from 240-900 ω_{pe}^{-1}; (b) corresponding hydrogen; and (c) oxygen phase space. The system is 240 λ_D long; timestep $\omega_{pe}\,\Delta t = 0.2$ and other parameters are given in the text.

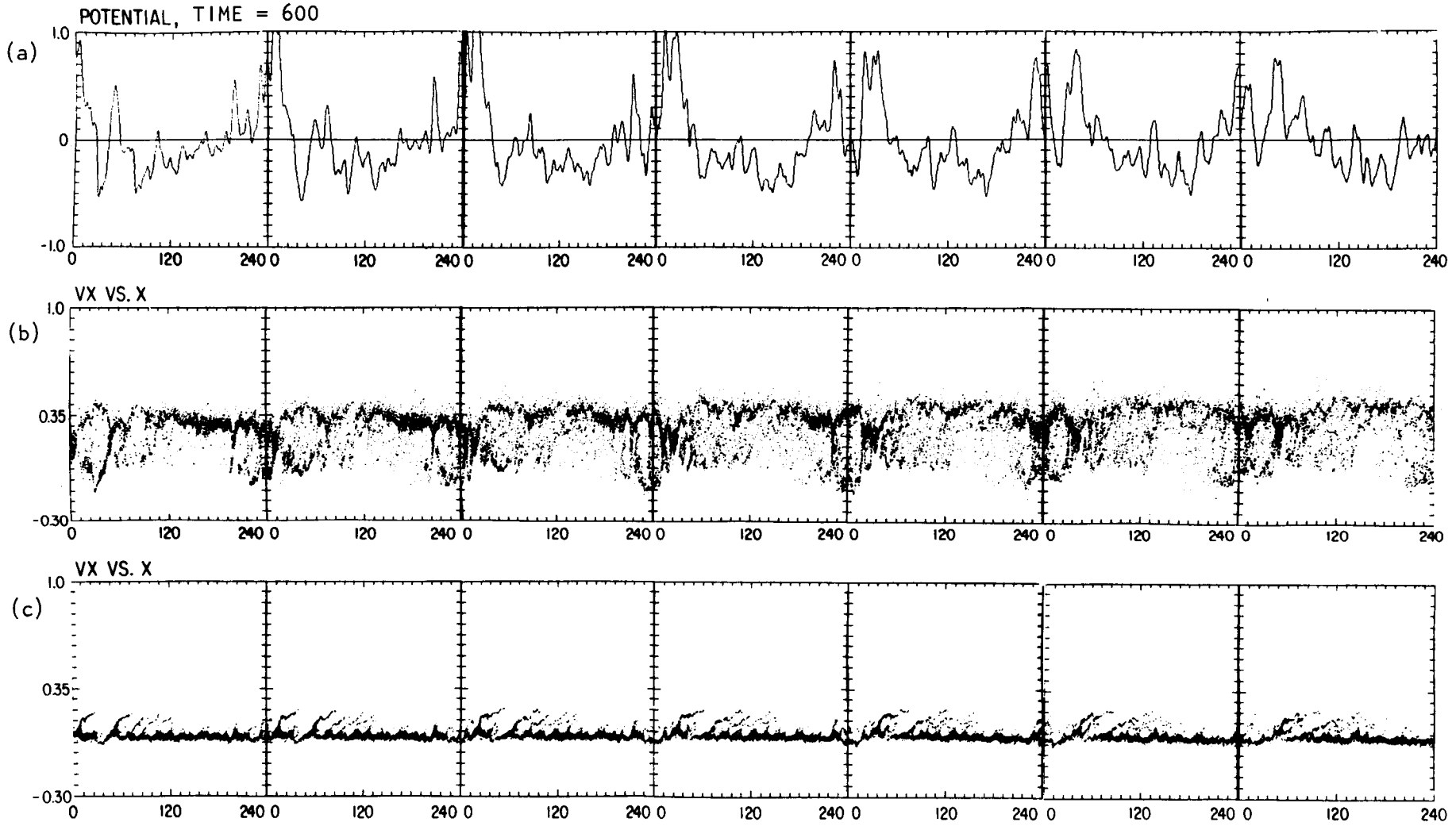

Figure 4. (Concluded)

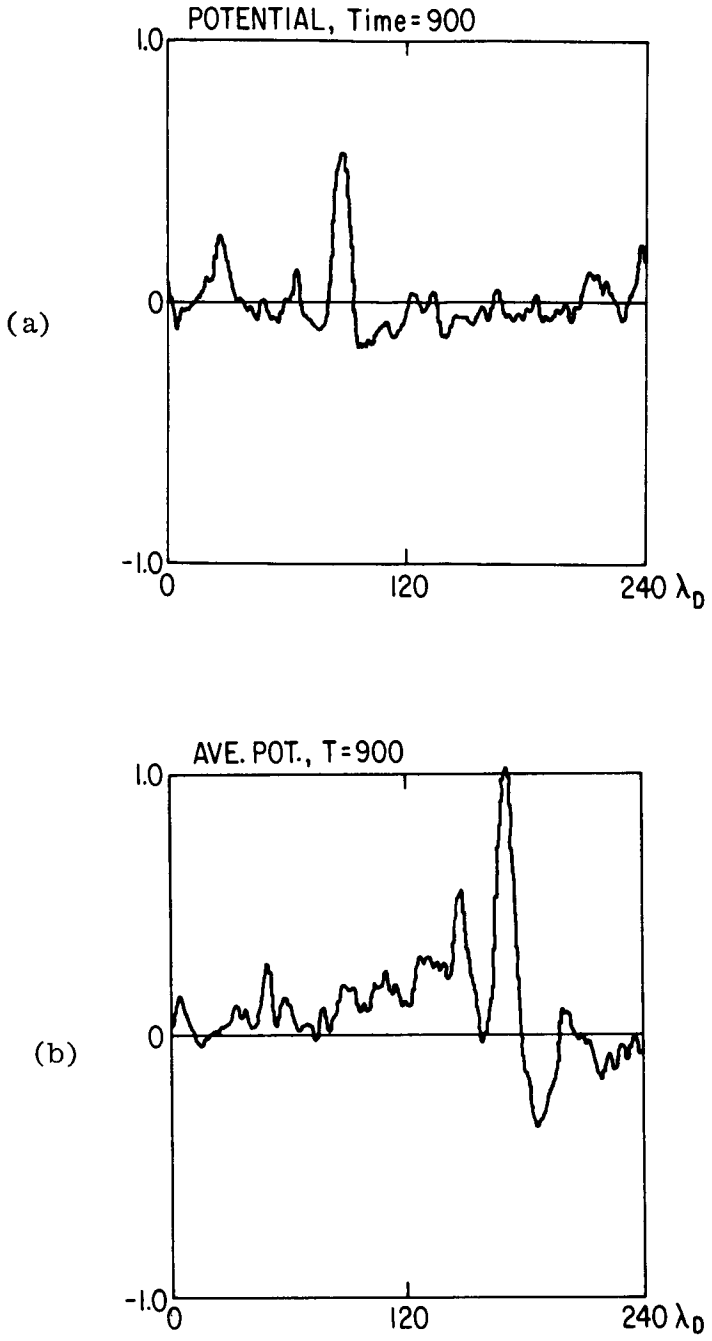

Figure 5. (a) Potential for run 7 at $\omega_{pe}\,\Delta t = 900$; (b) Potential for run 8 at $\omega_{pe}\,\Delta t = 900$. Parameters in (a) and (b) are the same, except that (a) was periodic, using ES1, and (b) was bounded using PDW1, with particle injection maintained constant as initialized ($V_H = 0.30$, $V_O = 0.06$, $V_e = 0$ in units of a_e) by an external circuit. All potential plots shown are averaged over 30 ω_{pe}^{-1}.

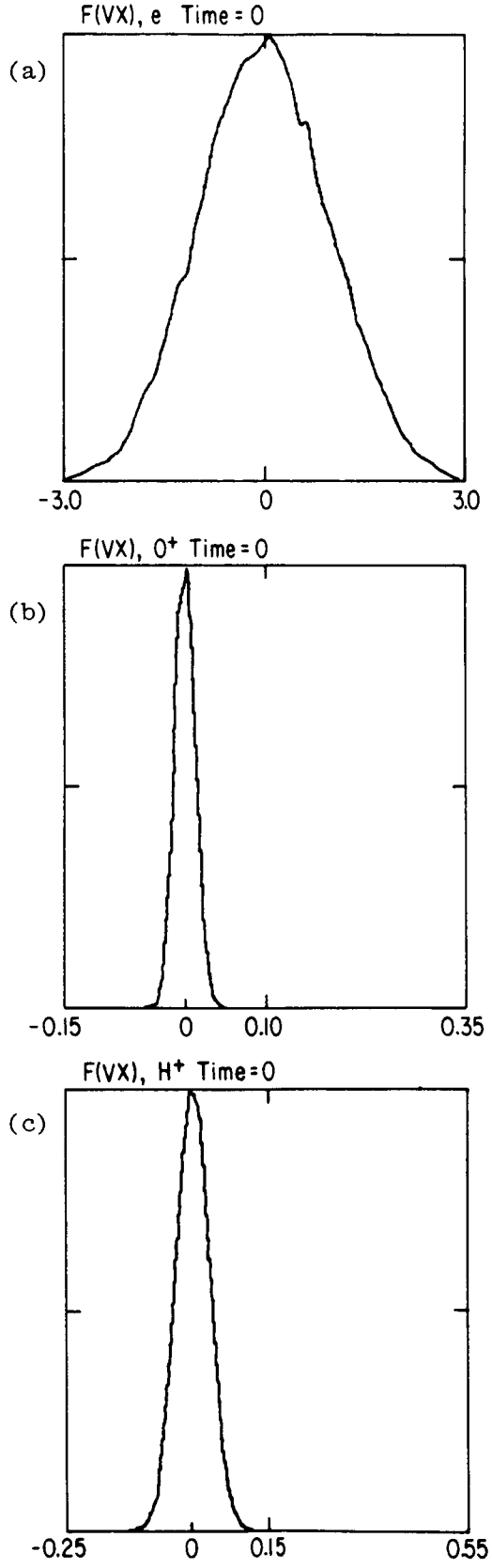

Figure 6. Initial (a) electron, (b) hydrogen, and (c) oxygen distribution functions for runs 9 and 10.

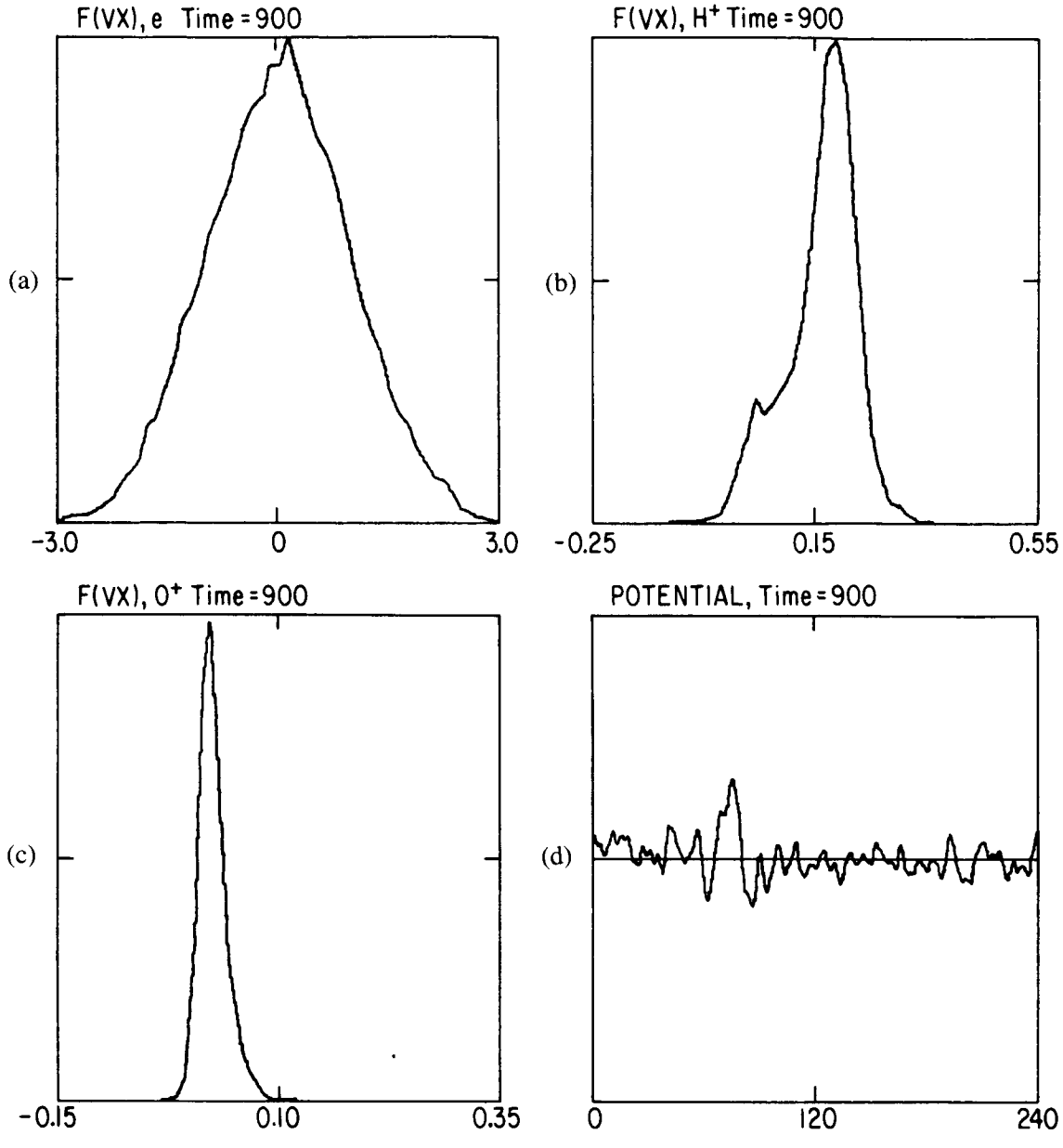

Figure 7. Same plots as Figure 6 for the stronger electric field case $eE_o/T_e = 2.4/240\ \lambda_D$, at the time an ion hole is beginning to form, $\omega_{pe}\ \Delta t = 900$. The potential averaged over 30 ω_{pe}^{-1} is also shown in (d).

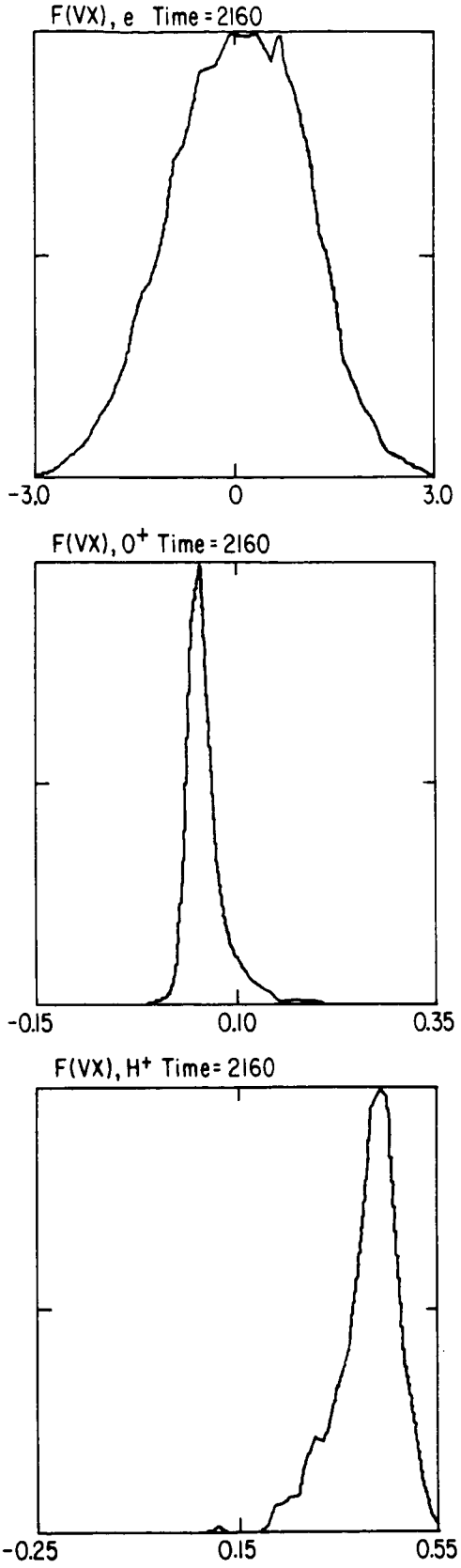

Figure 8. Same plots as Figure 6 for run 9 at $\omega_{pe}\,\Delta t = 2160$ when $V_H = 0.44\,a_e$ is becoming comparable to Figure 1.

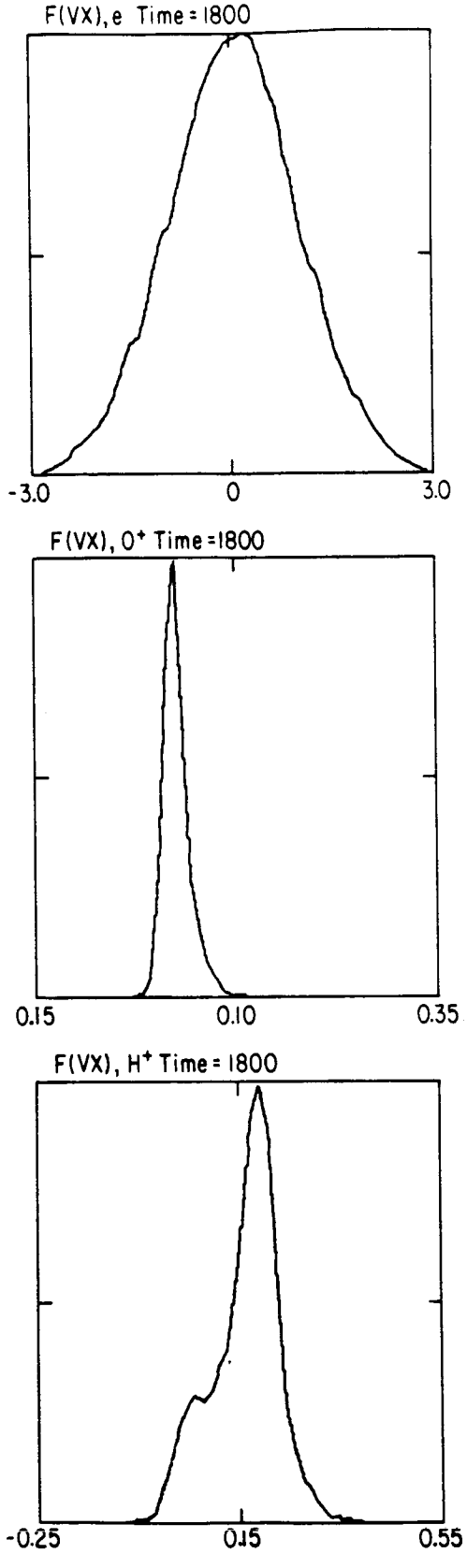

Figure 9. Same plots as Figure 6 for the weaker electric field case, run 10, with $eE_o/T_e = 1.2/240\ \lambda_D$, at $\omega_{pe}\ \Delta t = 1800$, corresponding to the same amount of ion acceleration as Figure 7.

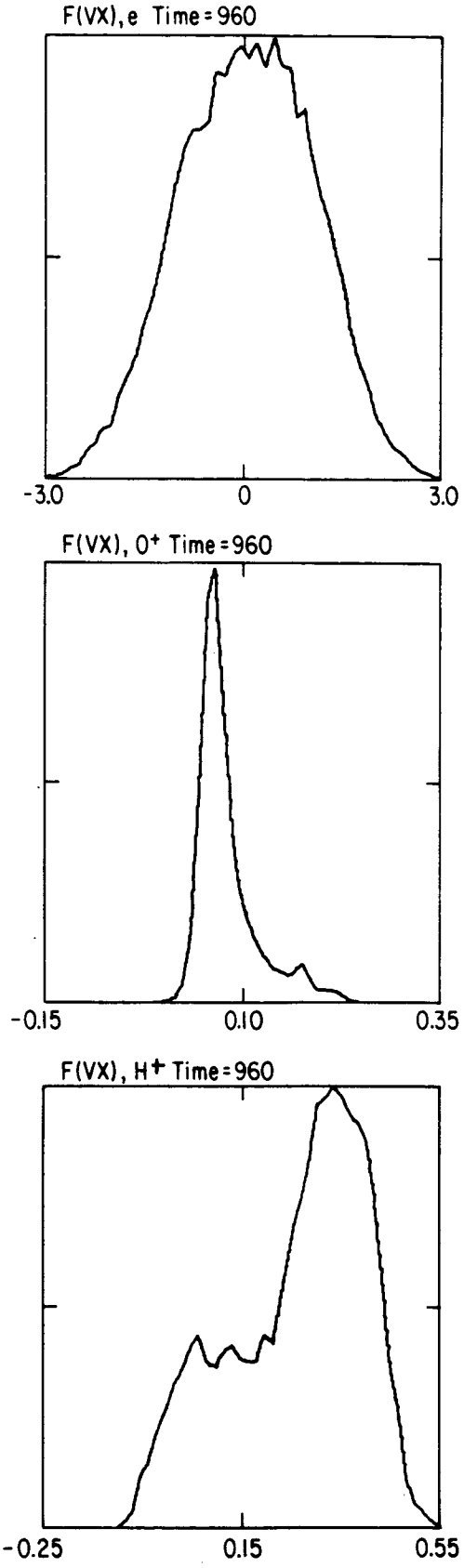

Figure 10. Same plots as Figure 6 for run 3, at the end of the time series shown in Figure 4.

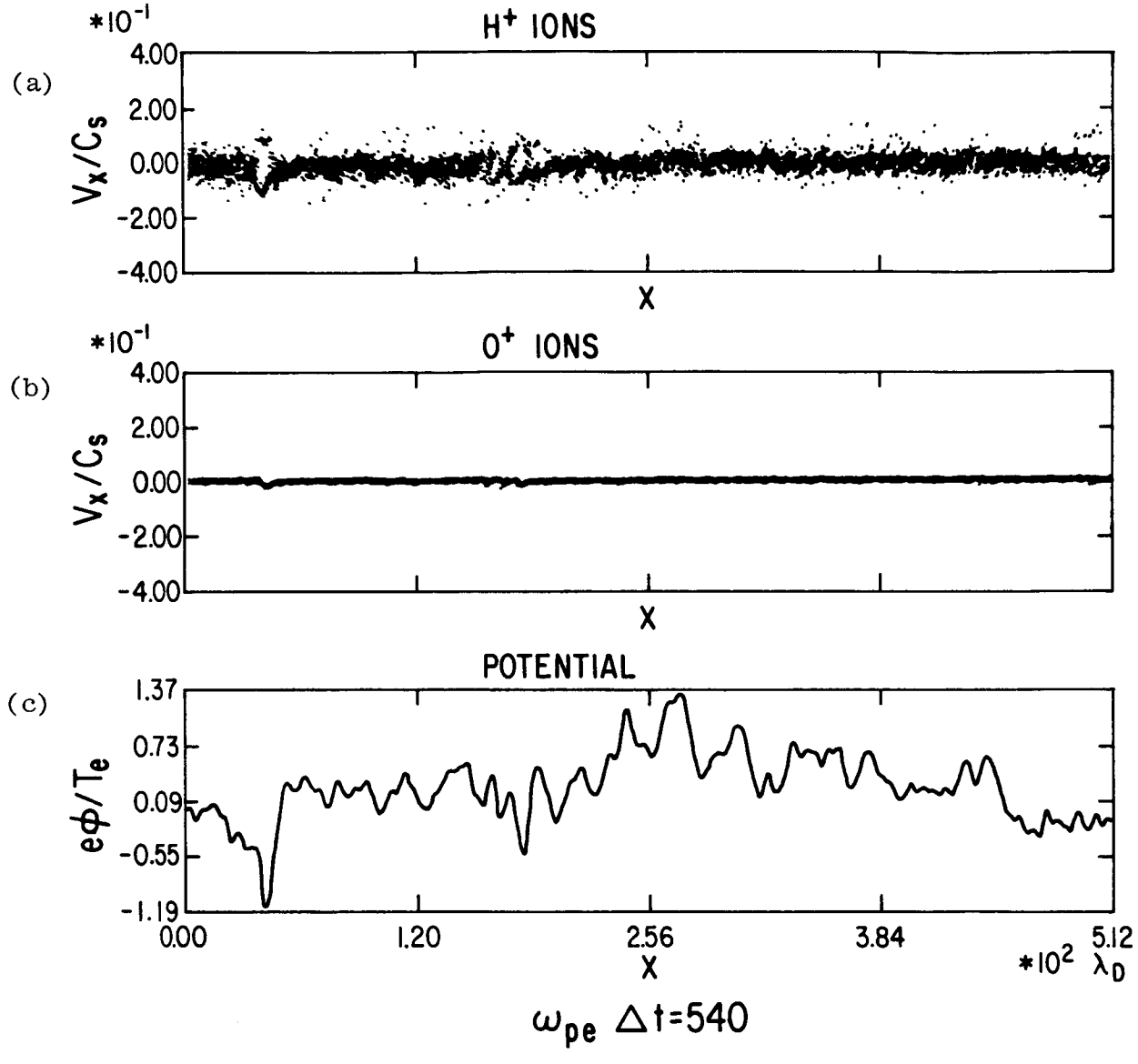

Figure 11. (a) Hydrogen and (b) oxygen distributions, and (c) potential averaged over 67.5 ω_{pe}^{-1} at $\omega_{pe}\,\Delta t = 540$. One or more double layers are apparent.

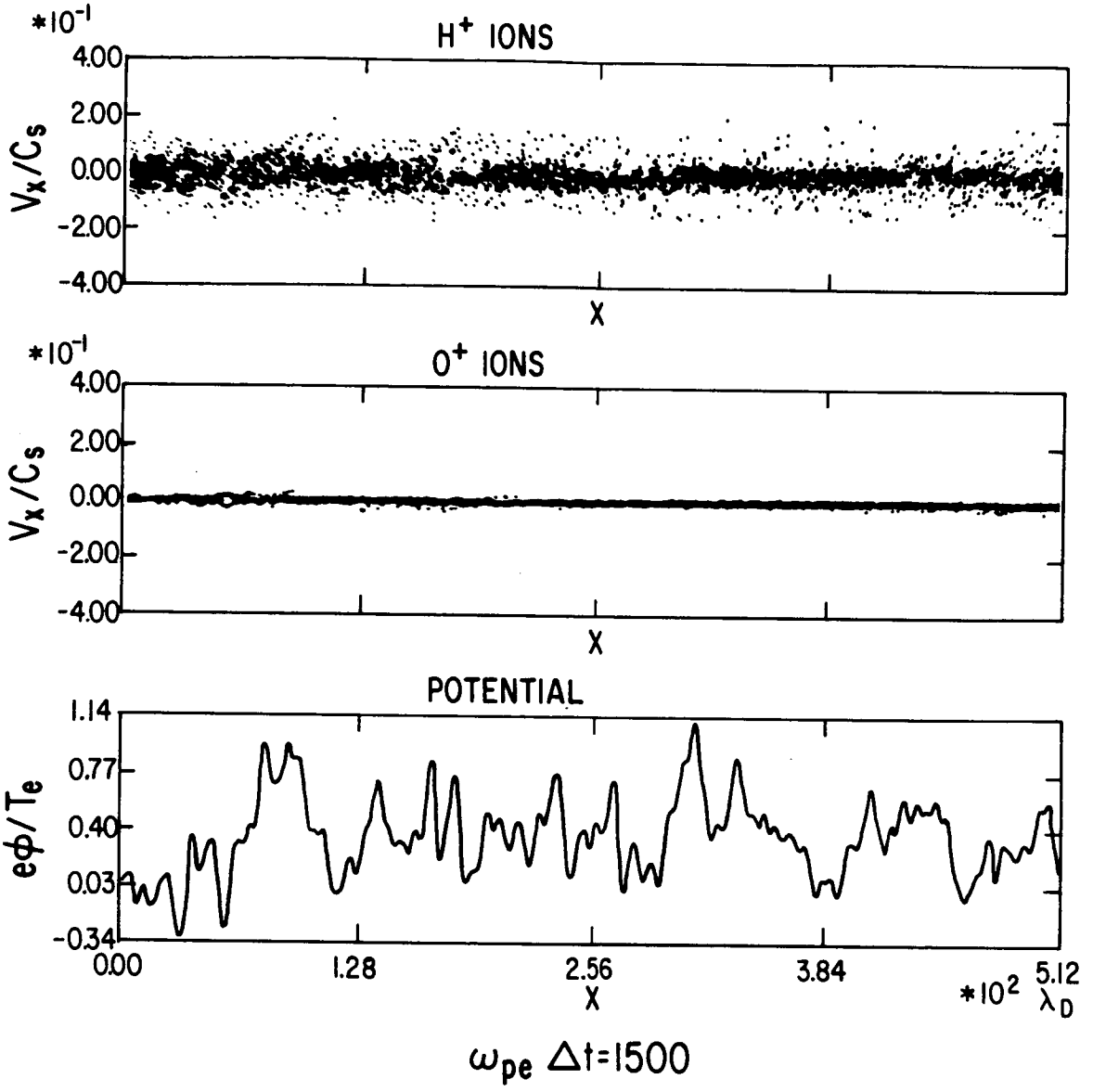

Figure 12. Same as Figure 11 at a later time $\omega_{pe}\,\Delta t = 1500$.